Journal Name

RSCPublishing

View Article Online
DOI: 10.1039/C4QI00128A

ARTICLE

Structural and biological study on new 3,5-diacetyl-1,2,4-triazol bis(*p*-chlorophenyl thiosemicarbazone) ligand and its bimetallic complexes†

Cite this: DOI: 10.1039/x0xx00000x

Received 00th January 2012,
Accepted 00th January 2012

DOI: 10.1039/x0xx00000x

www.rsc.org/

A.I. Matesanz,*[a] P. Albacete[a], J. Perles[b] and P. Souza[a]

Preparation and characterization of the new ligand 3,5-diacetyl-1,2,4-triazol bis(^{4}N-*p*-chlorophenylthiosemicarbazone), H_5L^1, and its bimetallic complexes $[Pd(\mu\text{-}H_3L^1)]_2$ and $[Pt(\mu\text{-}H_3L^1)]_2$, is described. The molecular structure of the complexes, determined by single crystal X-ray crystallography, reveals that each ligand coordinates, in an asymmetric dideprotonate form, to the metal ions in a square planar geometry. The new compounds synthesized have been evaluated for antiproliferative activity in vitro against NCI-H460, T-47D, A2780 and A2780*cis*R human cancer cell lines. The cytotoxicity data suggest that these compounds may be endowed with important antitumor properties, especially H_5L^1 since exhibit excellent antiproliferative activity surpassing the activity of cisplatin against three of the four tumor cell lines studied. The DNA binding ability of H_5L^1 and $[Pt(\mu\text{-}H_3L^1)]_2$ with calf thymus DNA in Tris-HCl buffer solution (pH=7.2) was explored by UV-Vis absorption spectroscopy and viscosity measurements. These data indicated that both compounds bind to DNA by a groove binding mode.

Introduction

Cisplatin is one of the most active chemotherapeutic agents available for the treatment of a number of solid tumors. The main cellular target of the drug is assumed to be DNA, specifically the formation of 1,2-intrastrand cross-link adducts that force the DNA to kink toward the major groove. These DNA distortions can effectively block the cell division and finally trigger cell death.[1-3]

Unfortunately the clinical utility of cisplatin is restricted due to the frequent development of drug resistance, the limited spectrum of tumors against which this drug is active and also the severe normal tissue toxicity. These disadvantages have driven the development of improved platinum-based anticancer drugs whose structure and mode of action differ from that of cisplatin, especially those that interact with specific molecular targets as for example are the processes associated to DNA: transcription, replication and repair.[4-8]

In this regard, of particular interest are compounds targeting ribonucleotide reductase (RR), enzyme that catalyzes the reduction of ribonucleotides to deoxyribonucleotides, which are the building blocks for the de novo DNA synthesis in all living cells. Cancer cells require increased RR activity to meet the demand for deoxyribonucleotides that are needed to support their rapid proliferation. Thus inhibition of RR activity leads to inhibition of DNA synthesis and repair, and also induces cell cycle arrest and apoptosis.[9-11]

The α-(N)-heterocyclic thiosemicarbazones have been reported to be among the most effective RR inhibitors yet identified. They constitute an important and versatile class of chelate ligands with highly interesting biological properties due to the important number of free ligands and derived metal complexes that have shown antimicrobial, antiviral or antitumor activity.[12-16] For thiosemicarbazone metal complexes multiple antitumor mechanisms of action have been proposed which in addition to the inhibition of RR include: a) covalent binding to the nitrogen bases of DNA hindering or blocking base replication, b)

creation of lesions in DNA strand by oxidative rupture and c) binding with DNA through non-covalent interactions such as H-bonding, intercalation, electrostatic interaction or groove binding.[17-21]

Investigations from our laboratory have led to the development of a series of 3,5-diacetyl-3,5-triazol bis(4*N*-monosubstituted thiosemicarbazones) and *in vitro* antiproliferative experiments have shown that some of them, particularly those bearing cyclohexyl, phenyl and tolyl groups exhibit important cytotoxic activity in various human cell lines derived from different types of solid tumors.[22-25] These results encouraged us to further investigate their antitumor properties as well as those of novel derivatives.

Thus, this work is aimed to describe the synthesis and chemical characterization of the new 3,5-diacetyl-1,2,4-triazol bis(4*N*-*p*-chlorophenylthiosemicarbazone) ligand, H_5L^1, and its bimetallic palladium(II) and platinum(II) complexes (Scheme 1).

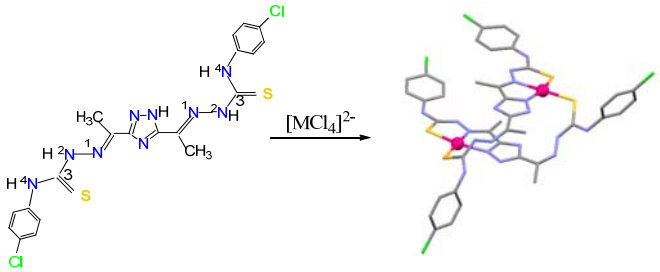

Scheme 1. Structure of the 3,5-diacetyl-1,2,4-triazol bis(4N-*p*-chlorophenylthiosemicarbazone) ligand and its metal complexes synthesized.

The cytotoxic activity of the new compounds synthesized, the related 3,5-diacetyl-1,2,4-triazol bis(4N-*p*-tolylthiosemicarbazone) ligand, H_5L^3, its platinum(II) derivative, di{3,5-diacetyl-1,2,4-triazol bis(4N-*p*-tolylthiosemicarbazonato) platinum(II)}, and cisplatin (assumed as the reference antitumor drug) has been studied against four human cancer cell lines: NCI-H460 (non-small cell lung cancer), T-47D (ductal breast epithelial cancer), A2780 and A2780*cis*R (epithelial ovarian cancer). DNA interactions abilities of H_5L^1 and $[Pt(\mu\text{-}H_3L^1)]_2$ have been investigated by absorption spectroscopy and viscosity measurements and also their binding constants (Kb) have been determined.

Results and Discussion

Synthesis and spectroscopic characterization

A new multidentate ligand, H_5L^1, has been synthesized with high purity and acceptable yield. This air and moisture stable yellow powder was obtained as monohydrate and was characterized by elemental analysis (C, H, N, S), mass spectrometry and IR and ^{1}H NMR spectroscopy.

The reaction of the flexible binucleating 3,5-diacetyl-1,2,4-triazol bis(4*N*-*p*-chlorophenyl thiosemicarbazone) ligand with $[MCl_4]^{2-}$ ions (M = Pd or Pt) led to the isolation of the neutral dimers complexes $[Pd(\mu\text{-}H_3L^1)]_2$ and $[Pt(\mu\text{-}H_3L^1)]_2$ in which each triazol-bis(thiosemicarbazone) behaves as dianionic ligand with deprotonation of one hydrazine (^{2}NH) and the triazole ring protons.

View Article Online
DOI: 10.1039/C4QI00128A

The air and moisture stable solids obtained were characterized by analytical and spectroscopic studies (selected IR and UV–VIS bands are listed in the Experimental section). The positive ionization mass spectra, ESI(+)-MS, in acetonitrile show a small peak at m/z = 1250.88 for $[Pd(\mu\text{-}H_3L^1)]_2$ and m/z = 1428 for and $[Pt(\mu\text{-}H_3L^1)]_2$ which confirm the 2:2 ligand to metal stoichiometry. As is shown in Figure 1, the experimental isotopic patterns of this ion fits perfectly with the theoretical mass distribution for proposed $[Pd(\mu\text{-}H_3L^1)]_2$ species.

The infrared spectral bands most useful for determining the mode of coordination of this ligand are the ν(C=N) iminic and ν(C=S) thioamide IV vibrations. However, the high delocalization and the asymmetric coordination only induce minor changes in these bands hindering the IR analysis. Specifically, in the spectra of metal complexes the ν(C=N) band appears slightly shifted to higher wavenumbers and the ν(C=S) thioamide IV band has decreased in intensity.

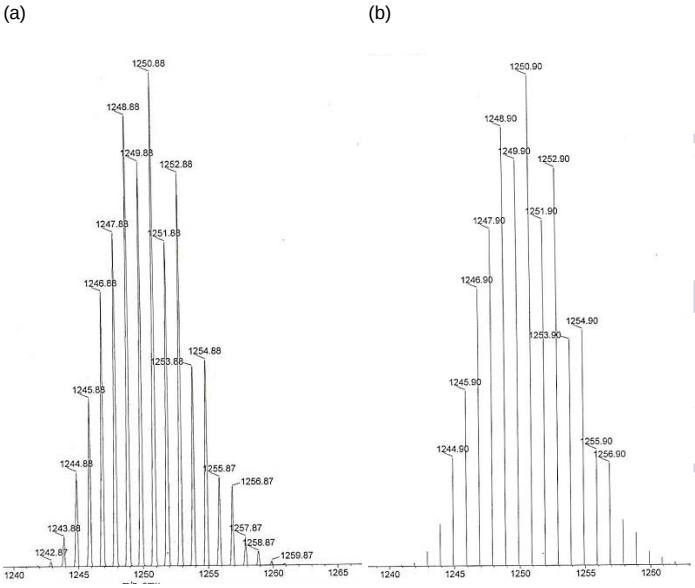

Figure 1. ESI(+)-MS spectra in acetonitrile solution of fragment $[Pd(\mu\text{-}H_3L^1)]_2^+$ a) experimental and b) theoretical isotopic distribution.

The ^{1}H NMR spectrum of the free ligand shows various peaks at low fields: δ = 14.75 ppm assigned to the triazolic proton, δ ~ 11.3 ppm assigned to the >C=N-^{2}NH- protons and δ ~ 10 ppm assigned to the –C(S)-^{4}NH- protons. In the ^{1}H NMR spectra of the complexes the absence of any signals above 13 ppm together with the presence of only one signal assigned to >C=N-^{2}NH- protons is consistent with the asymmetric dideprotonation of the ligands.

The electronic absorption spectra of both H_5L^1 ligand and $[Pd(\mu\text{-}H_3L^1)]_2$ and $[Pt(\mu\text{-}H_3L^1)]_2$ complexes exhibit two intense band in the region 250-400 nm, which can ascribed to ligand-centered n→π* and π→π* transitions. In addition the spectra of metal complexes exhibit other less energetic bands assigned to a ligand to metal (LMCT) and metal to ligand charge transfer (MLCT) transitions.[26]

Description of the crystal structures

Good quality crystals, suitable for single crystal X-ray diffraction analysis, were obtained for $[Pd(\mu\text{-}H_3L^1)]_2$ and $[Pt(\mu\text{-}H_3L^1)]_2$ compounds by recrystallization in dimethylsulfoxide (DMSO). The molecular structure of $[Pd(\mu\text{-}H_3L^1)]_2$ complex (Figure 2) consists of discrete $[Pd(\mu\text{-}H_3L^1)]_2\cdot 2.5DMSO\cdot H_2O$ molecules (the H atoms of the H_2O molecule were not located in the Fourier difference map).

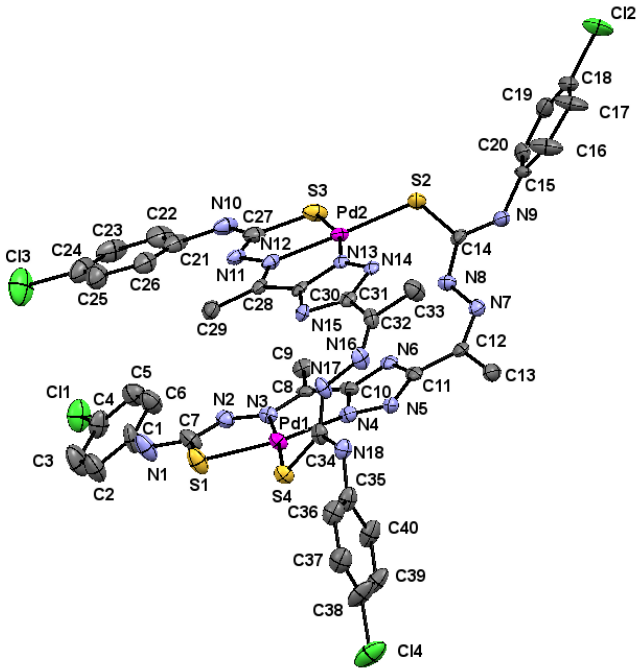

Figure 2. Molecular structure of the $[Pd(\mu\text{-}H_3L^1)]_2\cdot 2.5DMSO\cdot H_2O$ complex, hydrogen atoms and solvent molecules are omitted for clarity. The displacement ellipsoids are drawn at the 50% probability.

This neutral Pd(II) complex crystallizes in the monoclinic P21/n space group with Z=4 and its crystallographic analysis reveals unambiguously a dimeric structure, which results from the pairing of two metal centers through two thiosemicarbazone bridging moieties.

Each Pd(II) center is four-coordinated with a $[N_2S_2]$ donor environment, *via* one triazole nitrogen atom and the azomethine nitrogen, one sulfur atom belonging to the deprotonated arm of a ligand, and a sulfur atom from the neutral arm from the other ligand. Thus, the deprotonated thiosemicarbazone arm behaves as bidentate and the neutral one behaves as monodentate, acting the ligand as a bridge.

View Article Online
DOI: 10.1039/C4QI00128A

The bond angle data (Table 1) indicate that the stereochemistry around each palladium(II) ion is almost planar. The angles deviate slightly from that expected for a regular square–planar geometry, although this distortion may be attributed to the restricted bite angle of the tridentate moieties. Coordination results in the formation of two five-membered (PdSCNN and PdNCCN) chelate rings for each palladium(II) ion, which are coplanar with the deprotonated triazole ring.

Table 1. Selected bond distances and angles for $[Pd(\mu\text{-}H_3L^1)]_2\cdot 2.5DMSO\cdot H_2O$

Bond distances (Å)			
Pd1-S1	2.261(3)	Pd2-S2	2.316(3)
Pd1-S4	2.309(3)	Pd2-S3	2.268(3)
Pd1-N3	2.015(9)	Pd2-N12	2.012(9)
Pd1-N4	2.064(9)	Pd2-N13	2.080(9)
C7-S1	1.80(1)	C21-N10	1.441(17)
C14-S2	1.74(1)	C27-N10	1.345(15)
C27-S3	1.77(1)	C28-N12	1.295(14)
C34-S4	1.72(1)	C32-N16	1.289(15)
C7-N1	1.339(16)	C34-N18	1.353(14)
C7-N2	1.304(15)	N2-N3	1.359(13)
C8-N3	1.322(14)	N7-N8	1.403(13)
C12-N7	1.294(14)	N11-N12	1.386(12)
C14-N8	1.319(14)	N16-N17	1.402(13)
C14-N9	1.332(14)		
Bond angles (°)			
N3-Pd1-N4	80.6(3)	N12-Pd2-N13	79.7(3)
N3-Pd1-S1	83.8(3)	N12-Pd2-S3	84.0(3)
S1-Pd1-S4	91.9(1)	S3-Pd2-S2	92.2(1)
N4-Pd1-S4	103.7(3)	N13-Pd2-S2	104.0(2)
N4-Pd1-S1	164.4(3)	N13-Pd2-S3	163.7(3)
N3-Pd1-S4	175.6(3)	N12-Pd2-S2	176.2(3)

The Pd–N [2.012(9)-2.080(9) Å] and Pd–S [2.261(3)-2.316(3) Å] bond distances are slightly shorter than the sum of covalent radii of Pd and N or Pd and S (2.10 and 2.44 Å respectively) and are comparable with those reported for other Pd(II) thiosemicarbazone complexes.[24] It is important to note that upon coordination, the deprotonated arms undergo certain evolution from the thione to the thiol form [C7-S1=1.80(1) Å and C27-S3=1.77(1) Å], while the neutral thiosemicarbazone arms present shorter C–S bond lengths [C14-S2=1.74(1) Å and C34-S4=1.72(1) Å]. The C–N and N–N bond distances are intermediate between formal single and double bonds, pointing to extensive delocalization over the entire 3,5-diacetyl-1,2,4-triazole bis(thiosemicarbazone) skeleton.

Interestingly, the flexibility of the ligand originating from the free rotation of the two thiosemicarbazone arms allows each ligand the coordination to two metal ions in a twisted conformation generating two parallel coordination planes. The interplanar separation between the two triazole moieties is 3.302 Å, considered optimal for π-π interactions (intramolecular stacking).[27] This arrangement is reinforced by double intramolecular hydrogen bonds between the ^{2}NH of the bridging thiosemicarbazone moieties and the uncoordinated triazole nitrogen atoms.

The supramolecular association involves intermolecular hydrogen bonds between the ^{4}NH and the oxygen atoms from DMSO and water solvent molecules and the arrangement in the crystal can be described as a packing of columns of [Pd(μ-H_3L^1)]$_2$ molecules parallel to the [100] direction.

A drawing of complex [Pt(μ-H_3L^1)]$_2$·3DMSO is shown in Figure 3 and selected bond lengths and angles are given in Table 2.

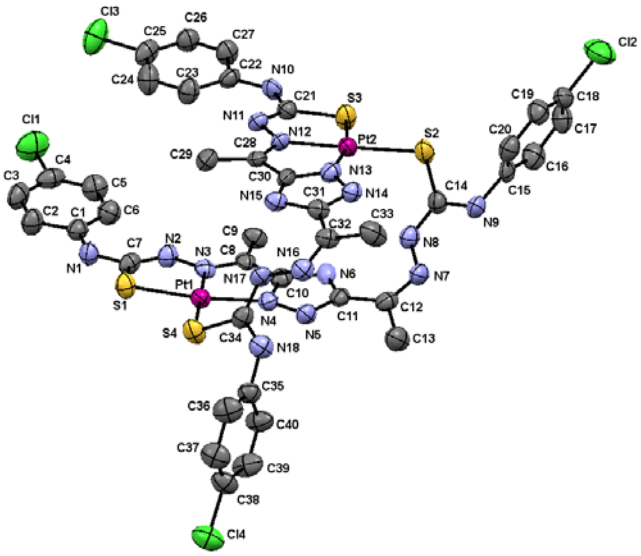

Figure 3. Molecular structure of the [Pt(μ-H_3L^1)]$_2$·3DMSO complex, hydrogen atoms and solvent molecules are omitted for clarity. The displacement ellipsoids are drawn at the 50% probability.

This dimeric compound crystallizes in the triclinic P-1 space group with Z=2. In a similar manner to the above described palladium dimer, the two 3,5-diacetyl-1,2,4-triazol bis(^{4}*N*-*p*-chloro phenylthiosemicarbazone) ligands coordinate in a bideprotonated form to the Pt(II) ions with one arm in a tridentate fashion (SNN) and with the other in a monodentate S-bridging mode.

The Pt-N and Pt-S bond distances are very similar to those found in [Pd(μ-H_3L^1)]$_2$ as would be expected based on the covalent radii similarity of palladium and platinum (1.39 and 1.36 Å respectively).

There is also a π-π interaction between the two triazole rings (centroids distance of 3.394 Å), as well as intramolecular hydrogen bonds involving the ^{2}NH of thiosemicarbazone moieties and the uncoordinated triazole nitrogen atoms. However, in this case, the two planes extend parallel up to the terminal phenyl rings so that a π-π stacking interaction between phenyl rings is also observed.

The supramolecular association is achieved through hydrogen interactions, between ^{4}NH and oxygen atoms from the DMSO molecules and the arrangement in the solid state can be described as a packing of columns of **[Pt(μ-H_3L^1)]$_2$** molecules parallel to the [010] direction.

These two structures with tridentate and monodentate bonding modes in the two arms, rather than bis-bidentate in both, result from the preferential binding of sulfur over nitrogen to palladium(II) and platinum(II) metal ions as well as the high stability of the tricyclic ring system of the tridentate moieties.

View Article Online
DOI: 10.1039/C4QI00128A

Table 2. Selected bond distances and angles for [Pt(μ-H_3L^1)]$_2$·3DMSO

Bond distances (Å)			
Pt1-S1	2.260(3)	Pt2-S2	2.281(3)
Pt1-S4	2.292(2)	Pt2-S3	2.250(2)
Pt1-N3	1.994(7)	Pt2-N12	2.000(8)
Pt1-N4	2.026(8)	Pt2-N13	2.017(7)
C7-S1	1.773(9)	C21-S3	1.75(1)
C14-S2	1.716(7)	C34-S4	1.73(1)
C7-N1	1.356(11)	C30-N15	1.343(11)
C7-N2	1.320(11)	C32-N16	1.272(10)
C8-N3	1.312(11)	C34-N17	1.321(10)
C12-N7	1.270(11)	C34-N18	1.338(11)
C14-N8	1.326(11)	N2-N3	1.383(10)
C14-N9	1.314(11)	N7-N8	1.391(10)
C21-N11	1.309(11)	N11-N12	1.393(9)
C28-N12	1.304(11)	N16-N17	1.385(10)
C30-N13	1.330(11)		
Bond angles (°)			
N3-Pt1-N4	79.5(3)	N12-Pt2-N13	79.8(3)
N3-Pt1-S1	84.6(2)	N12-Pt2-S3	84.7(2)
S1-Pt1-S4	94.7(1)	S3-Pt2-S2	95.08(9)
N4-Pt1-S4	101.3(2)	N13-Pt2-S2	100.5(2)
N4-Pt1-S1	164.0(2)	N13-Pt2-S3	164.4(2)
N3-Pt1-S4	179.2(2)	N12-Pt2-S2	178.9(2)

In vitro antiproliferative activity

To assess the antitumor potential of the synthesized compounds, its antiproliferative activity (in powder solid form) was tested *in vitro* against a panel of human cancer cells lines containing examples of lung (NCI-H460), breast (T-47D) and ovarian (A2780 and A2780cisR) cancers. For comparison purposes, the cytotoxicity of cisplatin was always evaluated under the same experimental conditions.

Out of an initial screening of the three compounds synthesized, both the free ligand and the platinum(II) derivative showed relevant antiproliferative activity with IC_{50} values falling in the low-micromolar range.

The remaining palladium(II) complex showed, at the maximum concentration tested of 100 mM, very low cellular growth inhibition (< 50%) and therefore its cytotoxicity could not be evaluated. IC_{50} values obtained for these two compound together with those for the related ligand 3,5-diacetyl-1,2,4-triazol bis(^{4}*N*-*p*-tolylthiosemicarbazone), H_5L^3, and its platinum(II) complex [Pt(μ-H_3L^3)]$_2$ are shown in Table 3. Specifically, the new ligand synthesized, H_5L^1, exhibit excellent antiproliferative activity surpassing the activity of cisplatin against three of the four tumor cell lines studied.

Table 3. *In vitro* antiproliferative activity of bis(thiosemicarbazone) compounds and cisplatin, evaluated in human NCI-H460 (non small lung cancer), T-47D (breast cancer), A2780 and A2780*cis*R (epithelial ovarian cancer) cell lines.

	IC_{50}±SD (μM)			
	A2780	**A2780*cisR***	**NCI-H460**	**T-47D**
H_5L^1	3.10±0.02	3.51±0.03	7.07±0.07	3.37±0.1
$[Pt(\mu\text{-}H_3L^1)]_2$	35±1	> 100	>100	49±1
H_5L^3	3.7±0.02[a]	3.8±0.4[a]	13±2[a]	5.33±0.05
$[Pt(\mu\text{-}H_3L^3)]_2$	2.6±0.04[a]	4.9±0.06[a]	6.3±0.26[a]	7.08±0.08
Cisplatin	0.88±0.01	7.77±0.10	7.25±0.56	12±1

The IC_{50} values are averages of two independent determinations.

[a] values taken from Ref. 23.

Of particular relevance is the value of the resistance factor, RF (defined as IC_{50} in A2780*cis*R / IC_{50} in A2780) of 1.1 versus 8.8 for cisplatin. An RF value of < 2 is considered to denote non-cross-resistance and therefore this compound is able to circumvent cisplatin resistance.[28,29] This ability to overcome cisplatin resistance in A2780cisR cells, agree with our previous studies on H_5L^3 suggesting that the mechanisms of resistance to cisplatin -most likely reduced drug transport, enhanced DNA repair and elevated GSH levels- are scarcely effective toward these 3,5-diacetyl-1,2,4-triazol bis(^{4}N-substituted-thiosemicarbazones). Upon complexation, the $[Pt(\mu\text{-}H_3L^1)]_2$ complex demonstrated moderate inhibitory effect against A2780 and T-47D cells while the related $[Pt(\mu\text{-}H_3L^3)]_2$ retained the activity in the four lines assayed. Interestingly, H_5L^1, H_5L^3 and $[Pt(\mu\text{-}H_3L^3)_{]2}$ compounds were more cytotoxic than cisplatin against T-47D cells.

DNA Interaction Studies

In order to initially address if any direct interaction with DNA is part of the mechanism of action of the compounds, UV-visible absorption spectra in absence and presence of calf thymus DNA (CT-DNA) were carried out for H_5L^1 and $[Pt(\mu\text{-}H_3L^1)]_2$ compounds.

Absorption spectral studies

The binding affinity between DNA and tested compounds can be detected by UV-Vis absorption spectroscopy by measuring the changes in the absorption properties of: a) DNA (for a variable compound concentration) or b) tested compound (for a variable DNA concentration).

The UV-Vis absorption spectrum of the typical B-form DNA exhibits a characteristic π→π* band at 260 nm as consequence of the chromophoric groups in purine and pyrimidine moieties. Compounds binding with DNA through intercalation are consistent with hypochromism (decrease in DNA band absorption), resulted of a stacking interaction between the aromatic ligand chromophore and the base pair of DNA. In case of compounds binding with DNA through external contact (including groove binding and electrostatic attraction) usually hyperchromism (increase in DNA band absorption) is observed which is attributable of a contraction and overall damage of the secondary structure of DNA.[30]

View Article Online
DOI: 10.1039/C4QI00128A

Thus, the absorption spectra of CT-DNA in presence of H_5L^1 and $[Pt(\mu\text{-}H_3L^1)]_2$ were recorded, by keeping constant CT-DNA concentration ($5.45x10^{-5}$ M) in diverse [CT-DNA]/[compound] mixing ratios and monitoring the change in the absorption intensity of the typical CT-DNA spectral band at 260 nm. As Figure 4 and 5 show, when the concentration of H_5L^1 or $[Pt(\mu\text{-}H_3L^1)]_2$ is gradually increased a significant increase in absorption of the DNA band occurs being the percentage of hyperchromism observed [% hyperchromism = ($A_{DNA\ bound}$ − $A_{DNA\ free}$) / $A_{DNA\ bound}$] about 22 % for H_5L^1 and 37 % for $[Pt(\mu\text{-}H_3L^1)]_2$.

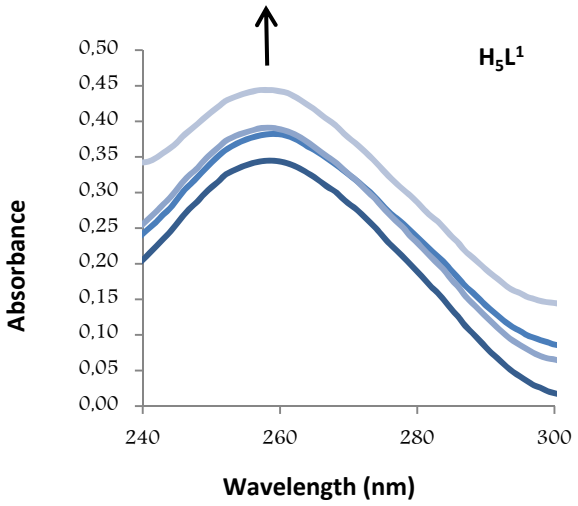

Figure 4. UV absorption spectra of CT-DNA in absence and presence of increasing amounts of compound H_5L^1 at diverse R values (R= [DNA]/[compound]): 0.0; 1.5; 2.0; 2.5.

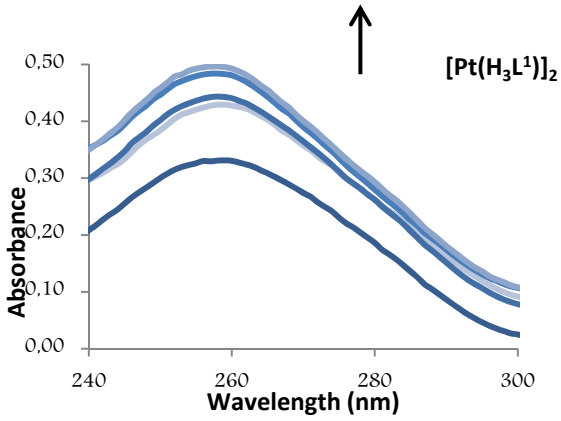

Figure 5. UV absorption spectra of CT-DNA in absence and presence of increasing amounts of compound $[Pt(H_3L^1)]_2$ at diverse R values (R= [DNA]/[compound]): 0.0; 3.0; 3.5; 4.0; 5.0.

The observed hyperchromic effect suggests that both compounds bind to CT-DNA by external contact. [31] These characteristics are comparable to those previously reported for

various neutral bis(thiosemicarbazone) palladium and platinum complexes and for which a non-covalent binding along outside of DNA helix surface (major or minor groove) was proposed.[24,32]

In the UV region, H_5L^1 and $[Pt(\mu\text{-}H_3L^1)]_2$ exhibit, in DMSO:Tris buffer (2.5:100) mixture, intense absorption bands attributable to intraligand transitions which could be perturbed in the case of interaction with CT DNA. Thus, in order to determine the intrinsic binding constant (Kb), absorption titration experiments were performed by maintaining a constant concentration of the desired compound while gradually increasing the concentration of CT DNA and monitoring the change in the absorption intensity of one of the intraligand charge transfer bands (for H_5L^1 ligand the band at λ_{max} 320 nm was used whereas for $[Pt(\mu\text{-}H_3L^1)]_2$ with less resolved bands the band at λ_{max} 255 nm was chosen). While measuring the absorption spectra, an equal amount of CT DNA was added to both the test solution and the reference solution to eliminate the absorbance of CT DNA itself. The data were then fitted to the following equation[33]:

$$\frac{[DNA]}{\varepsilon_a - \varepsilon_f} = \frac{[DNA]}{\varepsilon_b - \varepsilon_f} + \frac{1}{K_b(\varepsilon_b - \varepsilon_f)}$$

where [DNA] is the concentration of the nucleic acid in base pairs, ε_a is the apparent absorption coefficient obtained by calculating A_{obs}/[compound], and ε_f and ε_b are the absorption coefficients of the free and the fully bound compound, respectively.

A plot of [DNA]/(ε_a- ε_f) versus [DNA], gives a slope of 1/(ε_b- ε_f) and a Y-intercept equal to 1/{Kb(ε_b-ε_f)}. The intrinsic binding constant K_b is calculated as the ratio of the slope to the Y-intercept.

The UV spectra of H_5L^1 and $[Pt(\mu\text{-}H_3L^1)]_2$, Figures 6 and 7 respectively, display an increase in the absorptivity upon addition of increasing amounts of CT DNA (0 - 50 μM) which is indicative of interaction between the electronic states of the ligand chromophores with that of DNA bases.

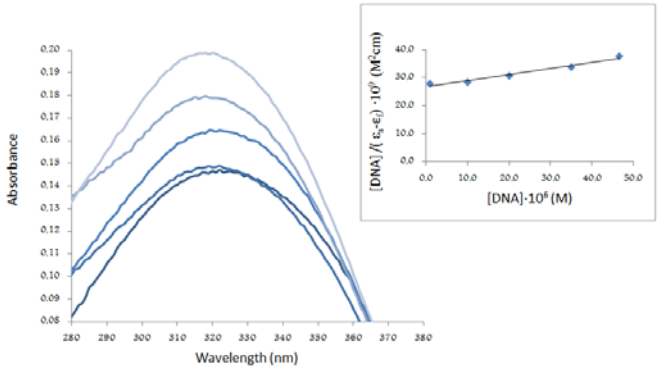

Figure 6. UV absorption spectra of H_5L^1 in presence of increasing amounts of CT-DNA. Data were collected for $[H_5L^1]$ = 5·10^{-6} M and [CT-DNA] = 1.25x10^{-6}, 5x10^{-6}, 20x10^{-6}, 25x10^{-6}, 50x10^{-6} M. The insert shows a fitting of the absorbance data used to obtain the binding constants.

View Article Online
DOI: 10.1039/C4QI00128A

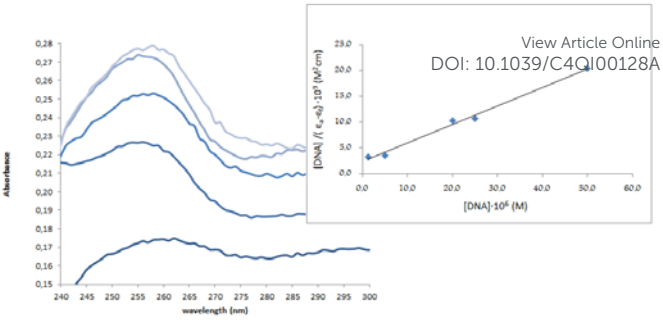

Figure 7. UV absorption spectra of $[Pt(\mu\text{-}H_3L^1)]_2$ in presence of increasing amounts of CT-DNA. Data were collected for $[Pt(\mu\text{-}H_3L^1)]_2$ = 5·10^{-6} M and [CT-DNA] = 1.25x10^{-6}, 5x10^{-6}, 20x10^{-6}, 25x10^{-6}, 50x10^{-6} M. The insert shows a fitting of the absorbance data used to obtain the binding constants.

This change in absorbance values was used to calculate the magnitude of intrinsic binding constant, K_b, for H_5L^1 and $[Pt(\mu\text{-}H_3L^1)]_2$ compounds, the values are 8.06x10^3 M^{-1} (correlation coefficient R^2 = 0.97) and 1.51x10^5 M^{-1} (correlation coefficient R^2 = 0.99) respectively.

The higher value of K_b obtained for $[Pt(\mu\text{-}H_3L^1)]_2$ in comparison to that calculated for the free ligand, H_5L^1, suggests that the coordination to Pt(II) ions enhance significantly the ability to bind to CT DNA. On the other hand, no significant shift is observed in the UV absorption band of the $[Pt(\mu\text{-}H_3L^1)]_2$ complex indicating that there is no change of the coordination environment of the metal ion and consequently discards covalent binding.

The K_g values obtained here are lower than that reported for double-stranded DNA intercalators while are comparable to other classical groove binders.[34,35] Therefore, these findings support the interaction of both compounds to DNA *via* groove binding.

Taking in account that both the free ligand and the platinum complex have demonstrated similar cytotoxic activity, it seems that DNA interactions is not the unique responsible for inhibition of cell proliferation. Further studies and more practical experiments are required to elucidate the biochemical mechanisms involved in their biological activity.

Viscosity measurements

Hydrodynamic methods such as determination of viscosity, which are fairly sensitive to the change of length of DNA, are also an important tool to study the nature of binding of compounds to the DNA. Thus, the potential interaction between H_5L^1 and $[Pt(\mu\text{-}H_3L^1)]_2$ compounds with DNA was examined further by viscosity measurements. Specifically, the relationship between the relative viscosity and the contour length is of the form $L/L_0=(\eta/\eta_0)^{1/3}$, where L_0 and η_0 denote the apparent DNA molecular length and the solution viscosity, respectively, in the absence of tested compound.

A classical intercalator molecule like ethidium bromide causes a significant increase in the viscosity of the DNA solution due to an increase in the separation of base pairs at the interaction

site and an increase in overall double helix length. Whereas a groove binder agent like Hoechst 33258 does not appreciably lengthen the DNA helix and therefore causes less pronounced changes (positive or negative) or no changes the viscosity of DNA solutions. On the other hand, cisplatin, which is known to fold DNA through covalent binding, causes a decrease in the relative viscosity of the DNA solution.[36]

The values of cube root of the relative specific viscosity, $(\eta/\eta_0)1/3$, versus the ratio of the complex concentration to DNA, 1/R (where R=[CT-DNA]/[compound]), in the absence and in the presence of compounds H_5L^1 and $[Pt(\mu\text{-}H_3L^1)]_2$ are plotted in Figure 8. Both compounds exhibit similar patterns: initially, at low concentration of compound, a clear diminution of the viscosity is observed suggesting a bending of the DNA chain probably due to strong hydrogen bonding interactions however, when the concentration of compound increase, a slight increase of the viscosity is observed pointing out to groove binding interactions as the dominant DNA interactions.[37,38] Thus, these results provide further support for the groove binding mode between these compounds and DNA.

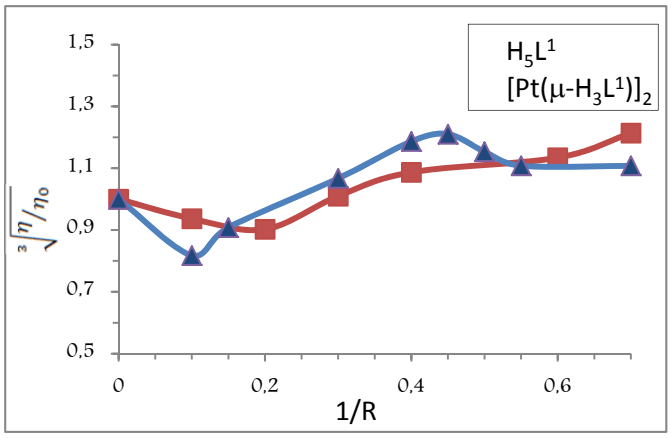

Figure 8. Effect of increasing amounts of compounds H_5L^1 and $[Pt(\mu\text{-}H_3L^1)]_2$ on viscosity of CT-DNA. The data were collected for [DNA] = 5.45×10^{-5} M at diverse 1/R ratios (R= [DNA]/[compound).

Experimental Section

Measurements

Elemental analyses were performed on a LECO CHNS-932 microanalyzer. Fast atom bombardment (FAB) mass spectrum (MS) was performed on a VG AutoSpec spectrometer and Electrospray Ionization (ESI) mass spectra were carried out on a QSTAR mass spectrometer. Nuclear Magnetic Resonance (NMR) spectra were recorded on a BRUKER AMX-300 spectrometer. All cited physical measurements were obtained out by the Servicio Interdepartamental de Investigación (SIdI) of the Universidad Autónoma de Madrid.

Melting points were determined with a Stuart Scientific SMP3 apparatus. The pH measurements were carried out with a Crison BASIC 20+ pH-meter equipped with a combined Crison glass electrode. Infrared spectra were recorded on a Bomen–Michelson spectrophotometer. Electronic spectra were recorded on a Thermo Scientific Evolution 260 Bio UV-visible (UV-VIS) spectrophotometer. Viscosity experiments were conducted on an automated AND viscometer model SV-1A.

View Article Online
DOI: 10.1039/C4GI00128A

Materials

Solvents were purified and dried according to standard procedures. Ultrapure MIlli Q water was used for all biological experiments. Hydrazine hydrate, L-lactic acid, *p*-chlorophenyl isothiocyanate, palladium(II) chloride, lithium chloride and potassium tetrachloridoplatinate(II) were commercially available.

Synthesis of compounds

3,5-diacetyl-1,2,4-triazol bis(^{4}N-*p*-chlorophenyl thiosemicarbazone) ligand, H_5L^1. An ethanolic solution (20 mL) of hydrazine hydrate (0.250 g, 5 mmol) was added dropwise with constant stirring to an ethanolic solution (20 mL) of p-chlorophenyl isothiocyanate (0.848 g, 5 mmol). The reaction mixture was stirred for one more hour and then the white product p-chlorophenylthiosemicarbazide formed was filtered, washed with cold ethanol and diethyl ether, dried *in vacuo* and recrystallized from ethanol. An ethanolic solution (20 mL) of the *p*-chlorophenylthiosemicarbazide (0.402 g, 2 mmol) was then refluxed with with 3,5-diacetyl-1,2,4-triazol (0,153 g, 1 mmol), which was previously described[39] , for five hours and then was left to stand to ambient temperature. The solution was reduced to half volume and the pale yellow solid formed was filtered, washed with cold ethanol and diethyl ether and dried *in vacuo*.

Yield (75%), mp 188 ºC. Elemental analysis found, C, 44.50; H, 4.15, N, 24.50; S 11.85; $C_{20}H_{19}N_9S_2Cl_2\cdot H_2O$ requires C, 44.61; H, 4.07, N, 24.22; S 12.32%. MS (FAB$^+$ with *m*NBA: nitrobenzyl alcohol matrix) *m/z* 520 (100%) for $[C_{20}H_{19}N_9S_2Cl_2+H]^+$. IR (KBr pellet): υ/cm^{-1} 3263 (s, NH-triazol), 3128 and 3089 (s, ^{2}NH and ^{4}NH), 1584 (m, CN), 756 (w, CS-thioamide IV band). ^{1}H NMR (300.14 MHz, DMSO-d_6): δ (ppm) 14.75 (s, NH-triazol, 1H), 11.30 (s, ^{2}NH, 1H), 11.29 (s, ^{2}NH, 1H), 10.23 (s, ^{4}NH, 1H), 10.00 (s, ^{4}NH, 1H), 7.68-7.28 (m, aromatic-thiosemicarbazide, 8H); 2.45 and 2.44 (s, CH_3-triazol, 3H).

Palladium(II) and platinum(II) complexes. Dinuclear [2+2] dimer complexes were obtained by reacting a methanol suspension (20 mL) of the 3,5-diacetyl-1,2,4-triazol bis(^{4}*N*-*p*-chlorophenylthiosemicarbazone) ligand with a methanolic solution (20 mL) of lithium tetrachloridopalladate (II) or a water solution (5 mL) of potassium tetrachloridoplatinate (II) in 1:1 molar ratios. The reaction mixture was stirred for 5 h at room temperature and the resulting orange solid obtained filtered, washed with methanol and diethyl ether, and dried *in vacuo*.

$[Pd(\mu\text{-}H_3L^1)]_2$. Yield (77%), mp 194 ºC (decomposes). Elemental analysis found, C, 33.55; H, 3.55, N, 18.00; S 9.10; C40H34N18S4Cl4Pd2·1010H2O requires C, 33.59; H, 3.78, N, 17.62; S 8.97%.g MS (ESI+ with CH3CN matrix) m/z 1250.90

for $[\{Pd(H_3L^1)\}_2+H]^+$. IR (KBr pellet): υ/cm^{-1} 3178, 3124, 3080 (s, ^{4}NH), 1592 (m, CN), 755 (vw, CS-thioamide IV band). ^{1}H NMR (300.14 MHz, DMSO-d_6): δ (ppm) 12.93 (s, ^{2}NH, 1H), 11.40 (s, ^{4}NH, 1H), 10.35 (s, ^{4}NH, 1H), 7.68-6.88 (m, aromatic-thiosemicarbazide, 8H); 2.46 (s, CH_3-triazol, 6H). Single orange crystals, suitable for single crystal X-ray diffraction, were grown by slow evaporation from a DMSO solution.

$[Pt(\mu\text{-}H_3L^1)]_2$. Yield (73%), mp 190 ºC (decomposes). Elemental analysis found, C, 30.10; H, 3.05, N, 15.70; S 7.85; $C_{40}H_{34}N_{18}S_4Cl_4Pt_2\cdot 10H_2O$ requires C, 29.89; H, 3.36, N, 15.69; S 7.98%. MS (ESI$^+$ with CH_3CN matrix) m/z 1428.03 for $[\{Pt(H_3L^1)\}_2+H]^+$. IR (KBr pellet): υ/cm^{-1} 3132, 3085 (s, ^{2}NH and ^{4}NH), 1585 (m, CN), 755 (vw, CS-thioamide IV band). ^{1}H NMR (300.14 MHz, DMSO-d_6): δ (ppm) 13.00 (s, ^{2}NH, 1H), 11.35 and 10.25 (s, ^{4}NH, 1H), 7.72-7.00 (m, aromatic-thiosemicarbazide, 8H); 2.49 (s, CH_3-triazol, 6H). Single orange crystals, suitable for single crystal X-ray diffraction, were grown by slow evaporation from a DMSO solution.

Single crystal X-ray diffraction

Data were collected on a Bruker Kappa Apex II diffractometer. Crystallographic data are listed in Table 4.

The software package SHELXTL was used for space group determination, structure solution, and refinement.[40] The structures were solved by direct methods, completed with difference Fourier syntheses, and refined with anisotropic displacement parameters. DMSO solvent molecules present a high degree of disorder, especially in the palladium derivative. The collection of diffraction data at 100 K did not improve this positional disorder.

In vitro antiproliferative activity

The human cancer cells: A2780 and A2780cisR (epithelial ovarian cancer), T-47D (breast cancer) and NCI-H460 (non-small cell lung cancer); were grown in RPMI-1640 medium supplemented with 10% foetal bovine serum (FBS) and 2 mM L-glutamine in an atmosphere of 5% CO_2 at 37 °C.

Cell proliferation was evaluated by the sulforhodamine B assay. Cells were plated in 96-well sterile plates at a density of $1.5x10^4$ (for NCI-H460), $4x10^3$ (for A2780 and A2780cisR) or $0.5x10^3$ (for T-47D) cells per well with 100µL of medium and were then incubated for 24 h (A2780, A2780cisR and NCI-H460) or 48 h (T-47D). After attachment to the culture surface the cells were incubated with various concentrations of the compounds tested freshly dissolved in DMSO (1 mg/mL) and diluted in the culture medium (DMSO final concentration 1%) for 48 h (for NCI-H460) or 96 h (for A2780, A2780cisR and T-47D). The cells were fixed by adding 50 µL of 30% trichloroacetic acid (TCA) per well.

The plates were incubated at 4 °C for 1 h and then washed five times with distilled water. The cellular material fixed with TCA was stained with 0.4% sulforhodamine B dissolved in 1% acetic acid for 10 min. Unbound dye was removed by rinsing with 0.1% acetic acid. The protein-bound dye was extracted with 10 mM unbuffered Tris base for determination of optical density (at 515 nm) in a Tecan Ultra Evolution spectrophotometer.

Table 4. Crystal and refinement data for $[Pd(\mu\text{-}H_3L^1)]_2\cdot 2.5DMSO\cdot H_2O$ and $[Pt(\mu\text{-}H_3L^1)]_2\cdot 3DMSO$

View Article Online
DOI: 10.1039/C4QI00020A

	$[Pd(\mu\text{-}H_3L^1)]_2\cdot 2.5DMSO\cdot H_2O$	$[Pt(\mu\text{-}H_3L^1)]_2\cdot 3DMSO$
Chemical formula	$C_{45}H_{49}Cl_4N_{18}O_{3.50}Pd_2S_{6.50}$	$C_{46}H_{52}Cl_4N_{18}O_3Pt_2S_7$
Formula weight	1461.01	1661.46
Temperature	100(2) K	296(2) K
Wavelength	0.71073 Å	0.71073 Å
Crystal size	0.02 x 0.02 x 0.21 mm	0.02 x 0.04 x 0.14 mm
Crystal habit	clear orange needle	clear orange prismatic
Crystal system	monoclinic	triclinic
Space group	$P2_1/n$	P-1
Unit cell dimensions	a = 8.123(3) Å b = 29.002(9) Å c = 28.87(1) Å α = 90° β = 93.92(2)° γ = 90°	a = 14.6278(2) Å b = 15.6060(2) Å c = 15.6896(3) Å α = 66.436(1)° β = 81.756(1)° γ = 68.305(1)°
Volume	6786.(5) Å^3	3050.39(8) Å^3
Z	4	2
Density (calculated)	1.430 Mg/cm^3	1.809 Mg/cm^3
Absorption coefficient	0.937 mm^{-1}	5.052 mm^{-1}
Theta range for data collection	1.41 to 25.33°	1.42 to 25.35°
Index ranges	$-9 \le h \le 9$ $-34 \le k \le 31$ $-34 \le l \le 26$	$-17 \le h \le 17$ $-18 \le k \le 18$ $-18 \le l \le 18$
Reflections collected	38026	79411
Independent reflections	12166 [R(int) = 0.0376]	11149 [R(int) = 0.0728]
Coverage of independent reflections	98.1%	99.7%
Data / restraints / parameters	12166 / 0 / 740	11149 / 0 / 731
Goodness-of-fit on F^2	1.048	1.032
Final R indices	9274 data; $I > 2\sigma(I)$ R_1 = 0.1086, wR_2 = 0.2948 all data R_1 = 0.1367, wR_2 = 0.3212	7715 data; $I > 2\sigma(I)$ R_1=0.0429, wR_2= 0.1108 all data R_1= 0.0807, wR_2=0.1439
Largest diff. peak and hole	6.233 and -2.253 eÅ^{-3}	2.893 and -2.688 eÅ^{-3}

The effects of compounds were expressed as corrected percentage inhibition values according to the following equation:

$$\%\ \text{inhibition} = \left(1 - \frac{T}{C}\right)\cdot 100$$

where T is the mean absorbance of the treated cells and C the mean absorbance in the controls.

The inhibitory potential of compounds was measured by calculating concentration–percentage inhibition curves, these curves were adjusted to the following equation:

$$E = \frac{E_{max}}{1 + \left(\frac{IC_{50}}{C}\right)^n}$$

where E is the percentage inhibition observed, E_{max} is the maximal effects, IC_{50} is the concentration that inhibits 50% of maximal growth, C is the concentration of compounds tested and n is the slope of the semi-logarithmic dose–response sigmoid curves. This non-linear fitting was performed using GraphPad Prism software.[41] For comparison purposes, the antiproliferative activity of cisplatin was evaluated under the same experimental conditions. All compounds were tested in two independent studies with triplicate points.

These experiments were carried out at the Unidad de Evaluación de Actividades Farmacológicas de Compuestos Químicos (USEF), Universidad de Santiago de Compostela.

DNA-Binding Experiments

CT-DNA stock solution was prepared by dissolving the lyophilized sodium salt in Tris-buffer (NaCl 50 mM, Tris-HCl 5 mM, pH was adjusted to 7.2 with NaOH 0.5 M) by stirring for 5 hours. The CT-DNA solution was standardized spectrophotometrically[42] by using its known molar absorption coefficient at 260 nm (6600 $M^{-1}\cdot cm^{-1}$). The ratio of UV absorbance at 260 and 280 nm, A_{260}/A_{280}, of *ca.* 1.9, indicating that the DNA was sufficiently free of protein. Stock solution was kept frozen until the day of the experiment.

Concentrated stock solutions ($5x10^{-3}$ M and $5x10^{-6}$) of H_5L^1 and $[Pt(\mu\text{-}H_3L^1)]_2$ compounds were prepared dissolving the compound in DMSO. From these stock solutions, for all experiments the desired concentration of compound was achieved by dilution with Tris-buffer (NaCl 50 mM, Tris-HCl 5 mM, pH was adjusted to 7.2 with NaOH 0.5 M) to give homogeneous solutions with DMSO content of less than 2,5 %.

To investigate the binding mode, spectrophotometric titrations were performed, at a fixed DNA concentration equal to $5.45x10^{-5}$ M, with increasing concentration of compounds (R=[CT-DNA]/[compound]) and monitoring the absorbance change at the wavelength maximum 260 nm after incubation (10 min. at 37ºC).

To calculate the binding parameters, the spectrophotometric titrations were performed with increasing concentration of DNA (0-50 μM) at a fixed compound concentration equal to 5 μM and monitoring the absorbance change in one characteristic charge transference band of the compound after incubation (10 min. at 37ºC).

The viscosity experiments were carried out, at constant temperature of 25.0 ± 0.1 ºC in a thermostated water bath using a water jacket accessory, at a fixed DNA concentration equal to $5.45x10^{-5}$ M with increasing concentration of compounds to ratios (1/R=[compound]/[CT-DNA]) in the range 0-0.7. For all of the experiments, the desired concentration of compound was achieved by dilution with Tris-buffer and DMSO to give homogeneous solutions containing a final concentration of 2.0 % of DMSO.

Conclusions

View Article Online
DOI: 10.1039/C4QI00128A

A new family of Pt(II) and Pd(II) bis(thiosemicarbazone) compounds of the 3,5-diacetil-1,2,4-triazol series containing an aryl ring with an electron withdrawing substituent (*p*-chlorophenyl group) has been successfully prepared and characterized.

According to the molecular structure, determined by single crystal X-ray diffraction, the two complexes display a dimeric structure as a result from the pairing of two metal centers through two thiosemicarbazone bridging moieties.

Investigation of potential biological properties (cytotoxicity and DNA binding studies) of the newly synthesized compounds indicated that H_5L^1 showed strongest antiproliferative activity surpassing the activity of the conventional standard cisplatin against three of the four tumor cell lines assayed. However $[Pt(\mu\text{-}H_3L^1)]_2$ complex exhibited better binding with CT-DNA which was inferred from the greater magnitude of the binding, in the range of classical groove binders. Thus our results suggest that non-covalent interactions with are not the unique molecular target for these compounds.

Acknowledgements

We are grateful to Ministerio de Economía y Competitividad, Instituto de Salud Carlos III (PI1100659), of Spain for financial support.

Notes and references

[a] Dpto. de Química Inorgánica (Módulo 07), Facultad de Ciencias, Universidad Autónoma de Madrid, c/ Francisco Tomás y Valiente nº 7, 28049-Madrid, Spain.
E-mail: ana.matesanz@uam.es

[b] Servicio Interdepartamental de Investigación (Módulo 13), Facultad de Ciencias, Universidad Autónoma de Madrid, c/ Francisco Tomás y Valiente nº 7, 28049-Madrid, Spain

† Electronic Supplementary Information (ESI) available: CCDC 997270 and 997271 contain the supplementary crystallographic data for [Pd(μ-H3L1)]2·2.5DMSO·H2O and [Pt(μ-H3L1)]2·3DMSO respectively. See DOI: 10.1039/b000000x/

1 F. Arnesano, M. Losacco, G. Natile, *Eur. J. Inorg. Chem*., 2013, 2701–2711.
2 J.D. Hoeschele, *Dalton Trans*., 2009, 10648-10650.
3 J. Reedijk, Eur. J. *Inorg. Chem*., 2009, 1303–1312.
4 N.J. Wheate, S. Walker, G.E. Craig, R. Oun, *Dalton Trans*., 2010, **39**, 8113-8127.
5 E. Wong, C.M. Giandomenico, *Chem. Rev*., 1999, **99**, 2451-2466.
6 Z. Guo, P.J Sadler, *Angew. Chem. Int. Ed*., 1999, **38**, 1512-1531.
7 M.S. Razzaque, *Nephrol. Dial. Transplant*., 2007, 1-5.
8 M. Okuda, K. Masaki, S. Fukatsu, Y. Hashimoto, K. Inui, *Biochem. Pharmacol.,* 2000, **59**, 195–201.
9 J. Shao, X. Liu, L. Zhu, Y. Yen, *Expert. Opin. Ther. Targets,* 2013, **17**, 1423-1437.

10 D.S. Kalinowski, D.R. Richardson, *Pharmacol. Rev*., 2005, **57**, 547–583.
11 C. Kunos, T. Radivoyevitch, F.W. Abdul-Karim, J. Fanning, O. Abulafia, A.J. Bonebrake, L. Usha, *J. Transl. Med*., 2012 10:79.
12 J.G. da Silva, L.S. Azzolini, S.M.S.V. Wardell, J.L. Wardell, H. Beraldo, *Polyhedron*, 2009, **28**, 2301-2305.
13 G.L. Parrilha, J.G. da Silva, L.F. Gouveia, A.K. Gasparoto, R.P. Dias, W.R. Rocha, D.A. Santos, N.L. Speziali, H. Beraldo, *Eur. J. Med. Chem.*, 2011, **46**, 1473–1482.
14 P. Genova, T. Varadinova, A.I. Matesanz, D. Marinova, P. Souza, *Toxicol. Appl. Pharmacol.,* 2004, **197**, 107-112.
15 P.J. Jansson, P.C. Sharpe, P.V. Bernhardt, D.R. Richardson, *J. Med. Chem.,* 2010, **53**, 5759–5769.
16 C.R. Kowol, R. Trondl, V.B. Arion, M.A. Jakupec, I. Lichtscheidl, B.K. Keppler, *Dalton Trans.,* 2010, **39**, 704-706.
17 A.I. Matesanz, P. Souza, *Mini-Rev. Med. Chem.,* 2009, **9**, 1389-1396.
18 S. Chandra, S. Parmar, Y. Kumar, *Bioinorg. Chem. & Appl*., 2009, ID 851316, doi:10.1155/2009/851316.
19 B. García, J. Garcia-Tojal, R. Ruíz, R. Gil-García, S. Ibeas, B. Donnadieu, J.M. Leal, *J. Inorg. Biochem*., 2008, **102**, 1892–1900.
20 F. Bisceglie, S. Pinelli, R. Alinovi, P. Tarasconi, A. Buschini, F. Mussi, A. Mutti, G. Pelosi, *J. Inorg. Biochem*., 2012, **116**, 195–203.
21 K. Abdi, H. Hadadzadeh, M. Salimi, J. Simpson, A. D. Khalaji, *Polyhedron,* 2012, **44**, 101–112.
22 A.I. Matesanz, Pilar Souza, *J. Inorg. Biochem*., 2007, **101**, 245-253.
23 A.I. Matesanz, C. Hernández, A. Rodríguez, P. Souza, *Dalton Trans*., 2011, **40**, 5738-5745.
24 A.I. Matesanz, C. Hernández, A. Rodríguez, P. Souza, J. Inorg. Biochem., 2011, **105**, 1613–1622.
25 A.I. Matesanz, J. Perles, P. Souza, Dalton Trans., 2012, **41**, 12538-12547.
26 A.A. Ali, H. Nimir, C. Aktas, V. Huch, U. Rauch, K. Schäfer, M. Veith, Organometallics, 2012, **31**, 2256–2262.
27 J. W. Steed, J. L. Atwood, in Supramolecular Chemistry, John Wiley & Sons, Chichester, second ed. 2009, pp 28-35.
28 L.R. Kelland, C.F.J. Barnard, K.J. Mellish, M. Jones, P.M. Goddard, M. Valenti, A. Bryant, B.A. Murrer, K.R. Harrap, Cancer Res., 1994, **54**, 5618–5622.
29 J. Ruiz, C. Vicente, C. Haro, D. Bautista, Inorg. Chem., 2013, **52**, 974–982.
30 F. Arjmand and M. Aziz, Eur. J. Med. Chem., 2009, **44**, 834–844.
31 P. Kalaivani, R. Prabhakaran, E. Vaishnavi, T. Rueffer, H. Lang, P. Poornima, R. Renganathan, V. Vijaya Padma, K. Natarajan; Inorg.Chem.Front., 2014, **1**, 311–324.
32 A.I. Matesanz, C. Hernández, P Souza, J. Inorg. Biochem., 2014, **138**, 16-23.
33 B. Pedras, R.M.F. Batista, L. Tormo, S.P.G. Costa, M.M.M. Raposo, G. Orellana, J.L. Capelo, C. Lodeiro, Inorg. Chim. Acta, 2012, **381**, 95-103.
34 H.K.H. Fong, B.R. Copp, Mar. Drugs, 2013, **11**, 274-299, doi:10.3390/md11020274.
35 N. Shahabadi, S. Hadidi, A. Taherpour, Appl. Biochem. Biotechnol., 2014, 172:2436–2454.
36 D. Suh, J.B. Chaires, Bioorg. Med. Chem. 1995, 3, 723-728.
37 E. Escribano, M. Font-Bardia, T. Calvet, J. Lorenzo, P. Gámez, V. Moreno, *Inorg. Chim. Acta,* 2013, **394**, 65-76.
38 J. Hernández-Gil, S. Ferrer, N. Cabedo, M.P. López-Gresa, A. Castiñeiras, F. Lloret, *J. Inorg. Biochem.,* 2013, **125**, 50-63.
39 C. D. Brandt, J. A. Kitchen, U. Beckmann, N. G. White, G. B. Jameson and S. Brooker, *Supramol. Chem*., 2007, **19**, 17–27.
40 SHELXTL-NT version 6.12, Structure Determination Package, Bruker-Nonius XS, Madison, Wisconsin, USA, 2001.
41 GraphPad Prism, version 2.01, GraphPad Software, Inc., San Diego, CA, 1996.
42 M.A. Ali, A.H. Mirza, A.L. Tan, L.K. Wei, P.V. Bernhardt, *Polyhedron,* 2004, **23**, 2037–2043.

COLOUR GRAPHIC

View Article Online
DOI: 10.1039/C4QI00128A

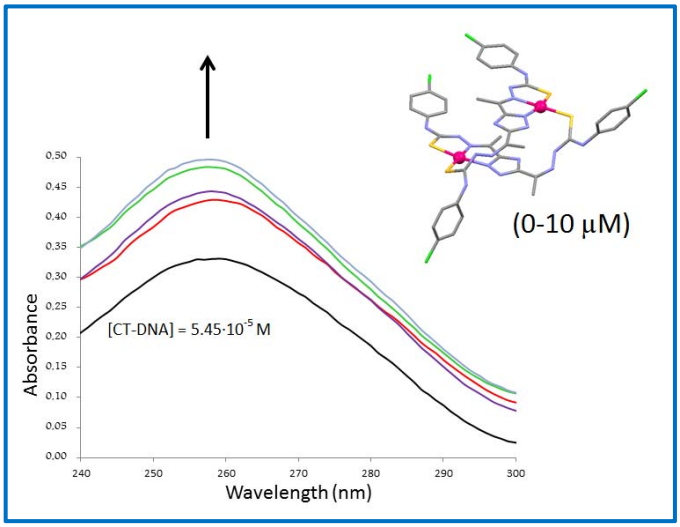

TEXT

Novel 1,2,4-triazole based bis(thiosemicarbazone) compounds with promising antitumor profile